ACCSCIENCE PUBLISHING

International Journal of Bioprinting

RESEARCH ARTICLE

3D printing of costal cartilage models with fine fidelity and biomimetic mechanical performance for ear reconstruction simulation

Senmao Wang[1], Di Wang[1], Liya Jia[2], Yuanzhi Yue[2], Genli Wu[2], Yuyun Chu[2], Qian Wang[1], Bo Pan[1], Haiyue Jiang[1]*, and Lin Lin[1]*

[1]Plastic Surgery Hospital, Chinese Academy of Medical Sciences and Peking Union Medical College, No. 33 Badachu Road, Shijingshan District, Beijing 100144, China

[2]3D Printing Laboratory, Elkem Silicones Shanghai Co Ltd, No. 515 Shennan Road, Minhang District, Shanghai 201108, China

Abstract

Patient-based training is difficult in ear reconstruction surgery; therefore, costal cartilage models are required for surgical education and pre-operative simulation. Here, we aimed to fabricate personalized models with mechanical and structural similarity to native costal cartilage to simulate ear reconstruction in microtia patients. To achieve this, the stiffness, hardness, and suture retention ability of both native costal cartilage and printed silicone were experimentally examined *in vitro*. Rheological tests and three-dimensional (3D) comparison methods were used to evaluate the printing ability and outcomes. The printed silicone models were used by residents to practice ear framework handcrafting during ear reconstruction surgery, and the residents' learning curves were analyzed. In addition, the models were used for pre-operative simulation to study and optimize the surgical plan. The results showed that the consistency of mechanical properties within cartilage and silicone was verified. Printable silicone had good shear-thinning properties, and the printed structures had almost perfect printing fidelity. Residents who used printed silicone models enjoyed great progress and confidence after training. The pre-operative simulation optimized the carving scheme, reduced trauma in the operative site, and avoided wasting necessary cartilage tissue. Overall, fine-fidelity models created in this study were intended for surgical education and pre-operative simulation by applying 3D-printable (3DP) silicone, facilitating the optimization of surgical plans. Surgeons were satisfied with this kind of model and recognized the efficacy and great application value of 3D-printed silicone models for clinical practice.

Keywords: 3D printing; Biomimetic model; Silicone; Surgical simulation; Costal cartilage

***Corresponding authors:**
Lin Lin
(linlin@psh.pumc.edu.cn)

Haiyue Jiang
(jianghaiyue@psh.pumc.edu.cn)

Citation: Wang S, Wang D, Jia L, *et al*., 2023, 3D printing of costal cartilage models with fine fidelity and biomimetic mechanical performance for ear reconstruction simulation. *Int J Bioprint*. https://doi.org/10.36922/ijb.1007

Received: May 27, 2023
Accepted: July 4, 2023
Published Online: August 3, 2023

1. Introduction

Microtia is a condition manifested as the partial or complete absence of external ear tissue, causing physical deformities and severe psychological burdens in millions of patients[1,2]. At present, autologous costal cartilage transplantation is the current

gold-standard therapy for such diseases because it is difficult for auricular cartilage tissue to repair or regenerate itself[3,4]. To successfully handcraft a realistic artificial external ear, surgeons should have a good understanding of the anatomy of the entire three-dimensional (3D) structure of an auricle and be capable of creating various aesthetic units of the external ear, including the helix, antihelix, superior and inferior crus, triangular fossa, and crus helix, through sculpture and suture[5]. However, ear framework fabrication remains a great challenge for residents who lack experience in practice. Performing procedures directly on patients is risky and may contribute to decreased therapeutic efficacy. Even experienced surgeons need pre-operative planning or simulated surgery to achieve satisfactory outcomes.

A critical challenge for surgical training and pre-operative simulation is to provide conditions for effective education without putting patients' health at risk[6]. A range of simulated handcrafting models offer a safe, nonclinical environment and immediate feedback designed to meet the educational needs of learners and the simulative needs of surgeons. Surgeons tried soap, fruits, and vegetables (e.g., carrots, apples, and potatoes) in early attempts to use simulated models because they were inexpensive and easy to obtain. Compared with soap, the mechanical properties of fruits and vegetables were significantly better for this purpose. However, fruits and vegetables were harder and less elastic and failed to mimic the shape of costal cartilage[7-9]. Then, surgeons started to work on the native cartilage harvested from the scapula and ribs of animal and human carcasses, which met the basic requirements for the mechanical properties and 3D structure. Nonetheless, in most cases, cartilage calcifications were observed in elderly cadavers. Moreover, the storage and application of isolated cartilage have some serious problems, such as high costs, the risk of spreading diseases, and related ethical issues[10]. Using synthetic polymer materials eliminated the problems of disease transmission and ethics. However, the problems with costal cartilage models made of manually cut rectangular polyvinyl chloride rubber or polyamide and starch include an unsophisticated morphological structure and unsatisfactory tear resistance of the surgical knot[11,12]. To accurately reproduce costal cartilage, some researchers injected polyurethane, vinyl polysiloxane, or silicone into computer-assisted fabricated negative impressions[13-15]. They replicated the shape of costal cartilage well. However, poor rigidity and strength kept them from imitating the texture of natural costal cartilage. Recently, we further produced costal cartilage models by indirect 3D printing that are satisfactory in subjective or even objective evaluation[16]. However, the fabrication of negative models makes the process tedious, which restricts pre-operative simulation because it requires personalized customized costal cartilage models for a large number of different patients.

Anatomical models created using 3D technology have become increasingly popular in clinical practice[17-19]. 3D-printed models provide unparalleled tactile perception and offer several advantages, such as being more cost-effective and accessible than traditional methods. In addition, these models can be customized to replicate specific anatomical structures or pathologies in life-sized models, making them a valuable tool in the education of surgeons and pre-operative simulation[20]. For instance, a randomized control trial suggests that 3D-printed models can be a more beneficial tool than cadaveric-based models for students[21] and a large number of applications of patient-specific 3D-printed models in cardiac surgical procedures[20,22].

Silicone (polysiloxane) has been widely used in various applications due to its biocompatibility and thermal stability[23], and altering the amount of these components can modify the mechanical and rheological properties of the silicone elastomer[24,25], which makes it attractive for mimicking biological tissue[26]. For example, in the field of facial plastic surgery, one significant application of silicone is in the fabrication of auricular prostheses[27,28]. Since the industrialization in 2015, material extrusion[29-32], vat photopolymerization[33,34], inkjet printing[35,36], and other technologies have been developed for the direct printing of silicones[37]. One of the most promising techniques to ensure high printing fidelity[38] is freeform additive manufacturing printing (FAM), defined as a variant of the material extrusion technique, which involves directly depositing liquid raw materials (generally termed "ink") into temporary or permanent supports[39-41]. The versatility of FAM technology and the unique properties of silicone make it an attractive combination for a wide range of applications in fields, such as biomedicine[42,43], soft robotics[44,45], and wearable devices[46,47]. The use of silicone in FAM has the potential to create complex, flexible, and biocompatible structures that cannot be easily produced with traditional manufacturing methods.

In this study, we aimed to use 3D-printable (3DP) silicone to fabricate biomimetic costal cartilage models. The mechanical properties of costal cartilage and these silicone materials, including hardness, stiffness, and suture retention ability, were comprehensively appraised *in vitro*. Then, rheological tests and 3D comparison methods are used to evaluate the printing performance of silicone materials. Finally, we used direct 3D printing biomimetic cartilage models in clinical practice to validate their value in surgery education and personalized surgical planning (Figure 1).

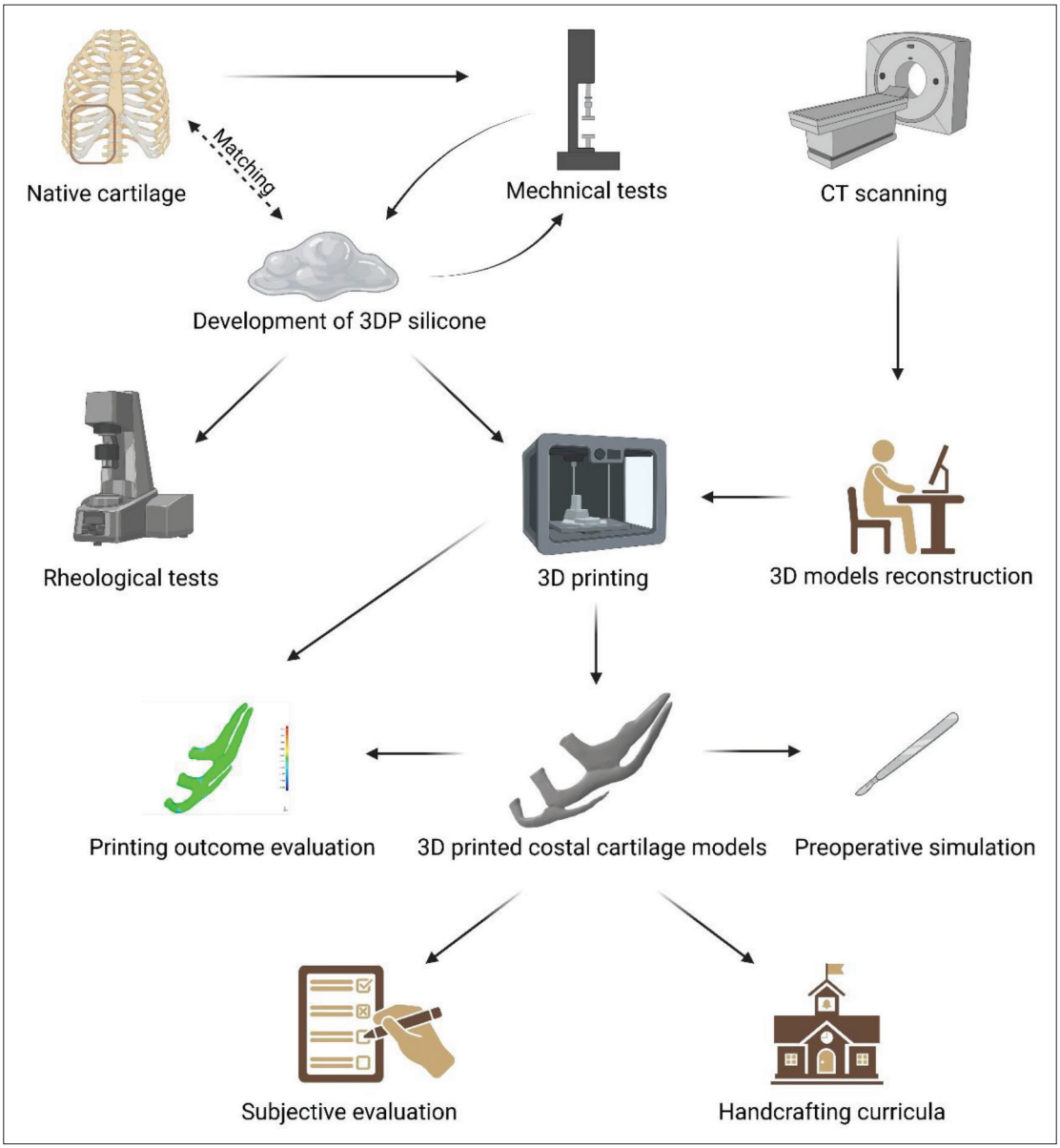

Figure 1. Schematic diagram of the fabrication and application of 3D-printable (3DP) silicone costal cartilage models. The discarded costal cartilage collected from the operation was matched with the printable silicone material according to the results of mechanical tests. Computed tomography (CT) scanning and 3D reconstruction provided personalized digital models of costal cartilage. The printed silicone models can be used for pre-operative simulation, surgical teaching, and receiving subjective evaluation feedback.

2. Material and methods

2.1. Materials and human tissue collection

Native costal cartilage pieces obtained from discarded postoperative tissue were used as the control material, and cartilage without calcification was included according to pre-operative computed tomography (CT) scanning. To obtain costal cartilage samples with desirable properties, the middle portion of the cartilage was utilized, while the perichondrium was removed as thoroughly as possible. The cartilage pieces were then immersed in 0.9% NaCl solution and stored at -80°C until testing[48]. To ensure complete thawing and stress equilibration, the samples were thawed before testing and then cut into their final shape. Using discarded postoperative tissue is a sustainable and ethical approach to using medical waste materials.

Three different types of two-component 3DP silicones and soluble supporting material were used in this study. The materials were provided by Elkem Silicones, Shanghai,

China, and detailed material formulations are shown in **Table S1** (silicone, Supplementary File) and **Table S2** (Supplementary File).

2.2. Mechanical and rheological tests

To comprehensively evaluate the mechanical properties of 3DP silicone as well as native costal cartilage, uniaxial compression tests, suture retention ability tests, and hardness tests were conducted. An additional uniaxial tension test was carried out for printed silicone materials. All harvested native costal cartilage samples were tested *in vitro*, and four samples from each printed silicone group were tested.

Uniaxial compression tests, uniaxial tension tests, and suture retention ability tests were performed on a universal testing machine (Instron 5967, Norwood, MA, USA) with a load cell capacity of 500 N. Cylindrical samples (2.2–9.2 mm in height and 5–6 mm in diameter) were isolated from native costal cartilage and printed silicone materials used for uniaxial compression tests (**Figure S1A** in Supplementary File and Figure 3A). Rectangular film samples (4 mm in width, 40 mm in length, and 2 mm in thickness) were cut from native costal cartilage (**Figure S2B** in Supplementary File) and printed silicone materials used for the suture retention ability test. According to the published method, a compression test was performed and analyzed[49]. A force of 10 mm/min was generally applied via the indenters to compress the specimens. In the undeformed state, the nominal stress was determined by the applied force divided by the cross-sectional area. The strain was determined by dividing the elongated sample length by the initial length. Young's modulus of costal cartilage was determined by the slope of the stress–stretch curve from the first approximate straight-line portion (**Figure S1A** in Supplementary File). Young's modulus was calculated from the stress–strain resistance data [stress (MPa) = load (N)/sample pressure sectional area (mm^2); strain (%) = compression displacement (mm)/sample compression plate height (mm)]. The suture retention ability test was conducted according to a previous study[50]. Instead of a suture line, a fine steel wire was used here to pierce the specimen at a distance of approximately 2 mm from both ends of the long axis, then the steel wire was fixed on the tension fixture, and the testing machine was run until the specimen was pulled out of a gap by the steel wire (**Figure S2B** in Supplementary File). The suture retention strength was determined by the maximal tensile force (**Figure S2A** in Supplementary File). Dumb-bell samples were cut into a specific size from printed silicone materials for the uniaxial tension test (Figure 3C).

Initial hardness was tested by a Shore durometer type A (Shahe®, Wenzhou, CHN) according to ASTM D2240. A cylindrical sample (5–10 mm in height and 5–6 mm in diameter) of each type of test material was prepared from printed silicone and native cartilage, with means measured at four different points in the sample. Within 1 s of completely pressing on the probe, data were recorded.

Rheology measurements were conducted using an MCR92 rheometer (Anton Paar, Austria). Components A and B were mixed homogeneously (1:1, volume ratio) with rapid manual stirring. The mixed material was transferred to a vacuum box and degassed for 30 min. Characterizations were performed just after mixing and degassing at 25°C. Shear viscosity (η) and shear stress (τ) sweeps were conducted as a function of shear rate (γ) between 0.1 and 100/s, which is typically encountered during extrusion-based processing.

2.3. 3D geometries and STL files

A CT scanner (Philips Healthcare, Netherlands) was used to collect images of the costal cartilage (6th to 8th rib) from microtia patients. 3D models of the collected costal cartilages were reconstructed and modified in 3D software (Mimics and 3-Matic, Materialise Inc., Leuven, BE). Then, all the data were converted into STL files.

2.4. 3D printing of costal cartilage models and other constructs

In this study, an S300 printer (San Draw, Taiwan, CHN) was used as the printing device for creating silicone costal cartilage models (**Table S3** in Supplementary File and Figure 2). The 3D printing device was a liquid extrusion molding system that featured a double-nozzle extrusion printing function. The main material used for printing was a two-component liquid silicone with Shore hardnesses of 65 A, 75 A, and 80 A, while the auxiliary soluble supporting material was also used. FAMufacture software (version 2.90; San Draw, Taiwan, CHN) is a customized software for printing operations and was used in this study.

We achieved 3D printing of STL models through the following operations:

(1) First, the printer was manually controlled by FAMufacture software to calibrate the platform;

(2) The printer was controlled by FAMufacture software to pre-extrude the material so that the nozzles can stably extrude the material;

(3) Data pre-processing: Magics software (Materialise Co. Ltd., Leuven, Belgium) was used to diagnose the data defect and repair the mesh error of the costal cartilage STL file and then export the new STL file;

(4) Molding position placement: the repaired costal cartilage STL file was imported into FAMufacture

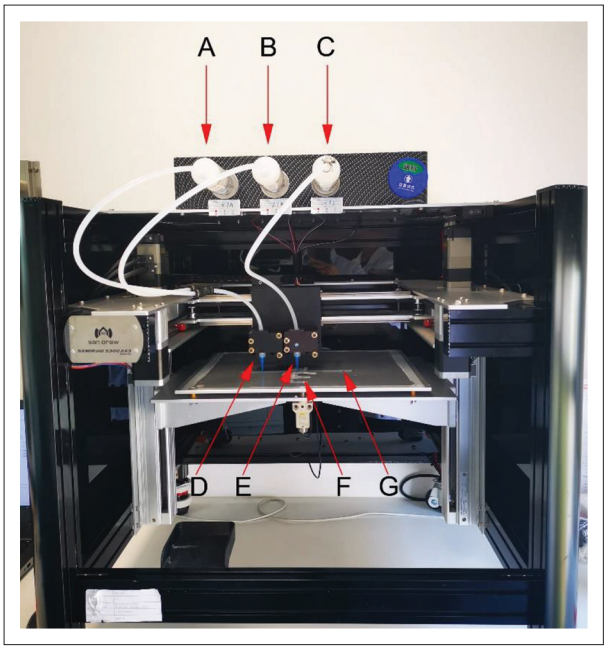

Figure 2. S300 3D printer. Carriers for storing silicone component A (A), component B (B), and supporting material (C). Printing nozzles of the mixed silicone (D) and supporting material (E). Costal cartilage model (F) and supporting structure (G) in printing.

software, and the molding direction and position of the model were adjusted;

(5) An extrusion nozzle of 0.4 mm and appropriate process parameters, such as scanning speed of 15 mm/s and layer thickness of 0.2 mm, were selected for parametric slicing using FAMufacture, with a 100% filling rate and 80% material supply rate, using the orthogonal scanning strategy [0°, 90°] for interlayer filling, directly slicing in FAMufacture, generating the Gcode print file, and then carrying out 3D printing.

After completion of the printing process, the printed silicone costal cartilage models were heated in a drying oven for 30–60 min at 80°C and then heated to 120°C for 15 min to complete post-curing of the printed constructs. Finally, the support materials were easily removed by flushing with water to prepare the final construct.

2.5. Printability outcome evaluation

To demonstrate the printability of the 3D printing technology used in this study, geometries with varying levels of structural complexity were examined, encompassing the production of auricular and nasal models.

The fidelity of the 3D-printed models was evaluated through a 3D comparison process. DICOM files of each printed model were obtained by CT and subsequently imported into Mimics for 3D reconstruction, resulting in the generation of STL files. The newly constructed 3D model files and the original digital model files were both input into Geomagic Control 2014 software (Geomagic, NC, USA). The initial digital model was set as the reference, while the newly built 3D reconstruction model was set as the test. The best-fit alignment method was used for automatic 3D matching, and we analyzed the morphological similarity of the two models by comparing the 3D deviation using deviation chromatograms. The same method was used for intergroup comparison of personalized printed models to evaluate the precision of the models.

2.6. 3D printing costal models for clinical practice (ear framework handcrafting curricula and pre-operative planning)

We assessed resident confidence in 10 learners who tried 3D-printed models using a retrospective scoring system[51,52]. Briefly, the learners rated their pre-training and post-training confidence levels after seven surgical simulations on a scale of 1 to 5, reflecting their confidence level changes and skill gains after practicing on costal cartilage models. To evaluate the effectiveness of the 3D-printed silicone models, each surgeon was asked to score their subjective impression of the models on a scale of 1 to 5 for hardness, elasticity, stickiness, suture-ability, and overall satisfaction, as shown in Table 1.

Enrolled patients for pre-operative simulation in the study were based on the following eligibility criteria: unilateral microtia, good health, no other chronic diseases except auricular deformity, and healthy costal cartilage without calcification or trauma. After manufacturing the 3D-printed silicone models, three senior plastic surgeons were invited to handcraft ear frameworks using the models, mainly according to the method reported in a previous study[53]. Surgeons optimized the harvesting and carving plan for costal cartilage based on personalized models pre-operatively and implemented the optimized protocol intraoperatively with maximal effort.

2.7. Statistical analysis

Continuous data were analyzed by the Kruskal–Wallis test (mechanical tests) or paired *t*-test (handcrafting curricula) or one-way ANOVA (Subjective evaluation). The level of significance was set at $p < 0.05$. Statistical analyses were conducted using GraphPad Prism 9.4 (San Diego, CA, USA).

3. Results and discussion

For the first time, we used a direct 3D-printing method to produce high-fidelity costal cartilage models with silicone as the raw material. The silicone materials in this study

Table 1. Subjective evaluation of experiences with costal cartilage models made by 3DP materials

	Costal cartilage	65 A	75 A	85 A
Hardness	5	4.77 ± 0.44	4.92 ± 0.28	4.85 ± 0.38
Elasticity	5	4.85 ± 0.38	4.85 ± 0.38	4.77 ± 0.44
Stickiness experienced during engraving	5	4.85 ± 0.38	4.77 ± 0.44	4.69 ± 0.48
Suture ability	5	4.92 ± 0.28	4.85 ± 0.38	4.38 ± 0.77
Overall satisfaction with the formed framework	5	4.92 ± 0.28	4.77 ± 0.44	4.62 ± 0.51
Total score	25	24.31 ± 1.03	24.1 ± 0.99	23.31 ± 1.18

Data are expressed as mean ± standard deviation.
Notes: 5, the same as costal cartilage; 1, sharply different from costal cartilage.

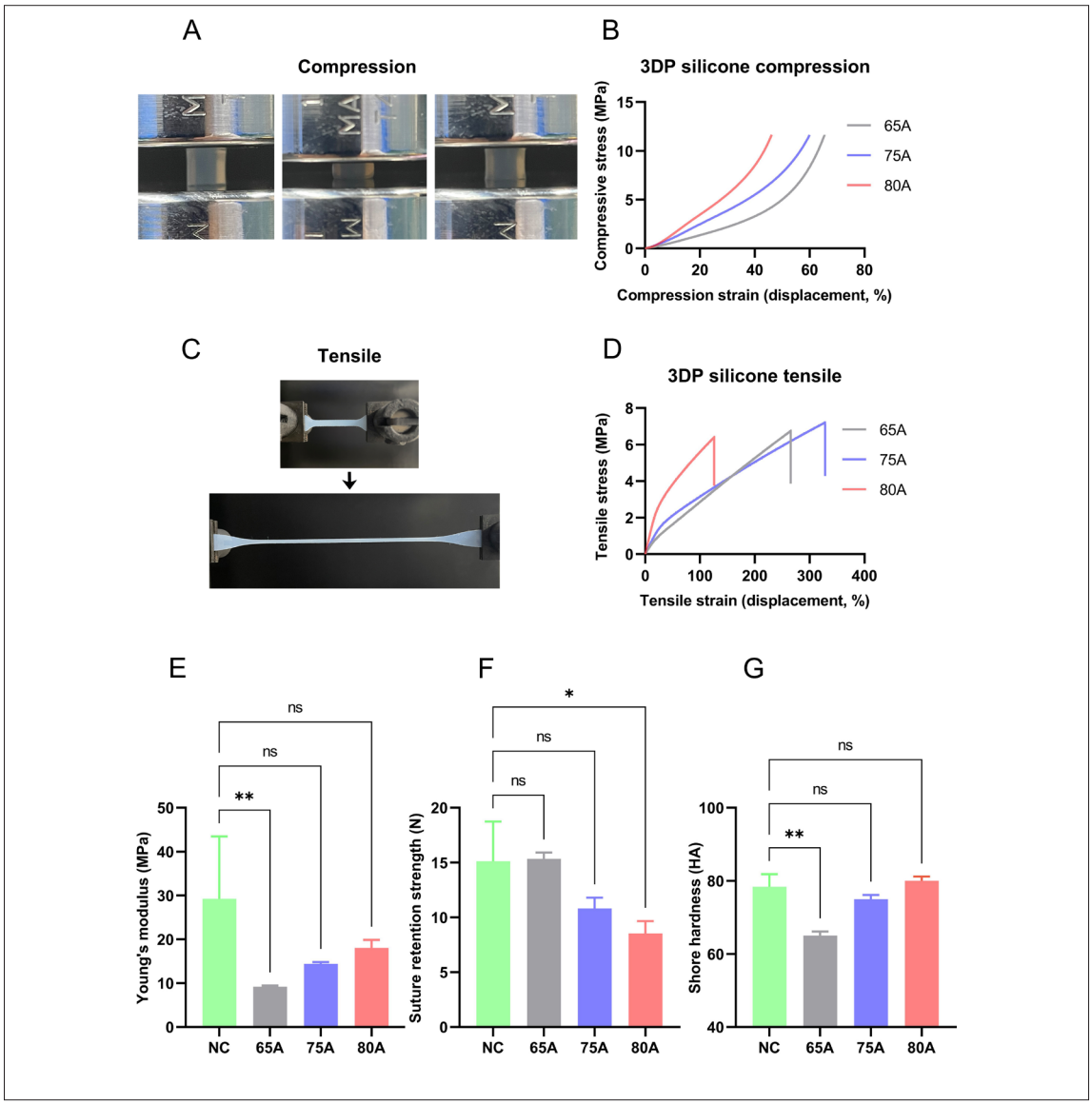

Figure 3. Mechanical properties of native cartilage (NC) and silicone materials. (A) Photographs of the compression test for the silicone materials. (B) Stress-strain results of the compression test. (C) Photographs of the tensile test for the silicone materials. (D) Stress-strain results of the tension test. Young's modulus (E), suture retention strength (F), and Shore hardness (G) of different silicone materials and native cartilage.
Notes: ns, no significant difference; *$p < 0.05$; **$p < 0.01$

were two-component liquid silicones. They consisted of two components that were mixed in equal parts. The curing mechanism was a hydrosilylation addition reaction. Siloxane containing Si–V bonds and siloxane containing Si–H bonds underwent hydrosilylation addition reactions under the action of platinum catalysts to crosslink. The material is available in various levels of Shore A hardness from 20 to 80. Based on our previous knowledge of costal cartilage hardness and our previous practice, 65 A, 75 A, and 80 A materials were developed for printing costal cartilage models, and they were printable through the method of extrusion.

3.1. Mechanical test of costal cartilage and printed silicone materials

The mechanical properties of costal cartilage in microtia patients were investigated. A total of 21 patients (7 females and 14 males) with an age range of 7–25 years were included in the study. The mean elastic modulus of costal cartilage was 29.25 ± 14.20 MPa, ranging from 9.67 to 67.02 MPa, and the mean hardness was 78.40 ± 3.46 A, ranging from 73 to 85 A, which is similar to the results of some previous studies[49,54,55] (**Table S4** and **Figures S3** and **S4** in Supplementary File).

Costal cartilage is a type of hyaline cartilage that connects the sternum and ribs and exhibits viscoelastic behavior[56]. The modulus of costal cartilage varies with time, degree of deformation, remodeling, and the geometry of forces applied. This variation is due to the structural complexity and anisotropy[57]. Then, the subjective nature of the modulus determination method must be acknowledged and may result in a certain degree of error. Our study focused on patients undergoing surgery for microtia, with a small age range of 7–25 years, and 19 of total 21 of them were minors. The smaller age difference in cartilage origin may be the reason no association was found (**Figures S3** and **S4** in Supplementary File) compared with previous research[56]. While the mechanical properties of costal cartilage may be influenced by calcification[55], which tends to increase with age[58], patients with calcified cartilage were excluded from the study, and previous research has indicated that the rate of calcification in costal cartilage among individuals in this age group is low[59]. Therefore, it is considered that calcification does not significantly impact the results of this test.

Figure 3B and D show the results of compression and tension tests for three different printed silicones. The mechanical properties of different costal cartilage models were further comprehensively evaluated and compared to test their potential as a mimicking curving tool. No significant difference in Young's modulus and Shore hardness was observed between the costal cartilage and 75 A and 80 A silicone materials. As a measure of a material's stiffness, Young's modulus measures an object's ability to resist deformation[60]. Indentation or abrasion can cause localized plastic deformation, which is measured as hardness. Cutting and stabbing would be extremely difficult if a model exceeds the hardness of the native cartilage. In contrast, an oversoft material would relax the indentation stress rapidly and cause viscous hysteresis during cutting. The results indicated that the 75 A and 80 A materials are flexible enough and would not easily deform with suitable hardness similar to native cartilage. Ear frameworks are stitched together with wires, and suture retention ability is essential in determining how difficult it is to suture the ear and whether the connection is firm enough. The results showed that the performance of 65 A and 75 A materials was comparable to native cartilage (Figure 3E–G). Although there was no significant difference in suture retention ability or Young's modulus between the 65A material and costal cartilage, the hardness of the 65A material was lower than that of costal cartilage. On the contrary, although there was no significant difference in hardness between the 80 A material and costal cartilage, there is an insufficiency of suture retention ability, which would lead to insecure connection. Based on the present data, the 75 A material showed no significant difference from native cartilage in objective evaluation and could be the best choice as a simulation material.

3.2. Rheological behavior and printability of 3DP silicone

Figure 4D–F display the rheological curves of 3DP silicone. At the lowest evaluated shear rate (0.1/s), 65 A, 75 A, and 80 A materials recorded viscosities of 2076.8, 2428.5, and 2935.9 Pa·s, respectively, and demonstrated shear-thinning (pseudoplastic) behavior. At lower shear rates, the pseudocrosslinking phenomenon caused by the van der Waals force between SiO_2 particles and polydimethylsiloxane (PDMS) molecular chains made the composites exhibit higher viscosity[61]. As the shear rates rose from 0.1 to 100/s, the pseudocrosslinking structure was gradually destroyed, and the PDMS molecular chains relaxed, which caused the viscosity of the composites to decrease, and the material exhibited a drop in viscosity to 13.9, 9.2, and 20.8 Pa·s, respectively; moreover, the relationship between them was a power function during this period. The three formulations showed fair rheological properties, which indicate low viscosity before curing and capacity for shear thinning.

The anatomical structures of the ear and nose were well represented, and the costal cartilage with special-shaped structures can also be printed (Figure 4A–C). Generally, the influence of gravity may lead to the collapse of the

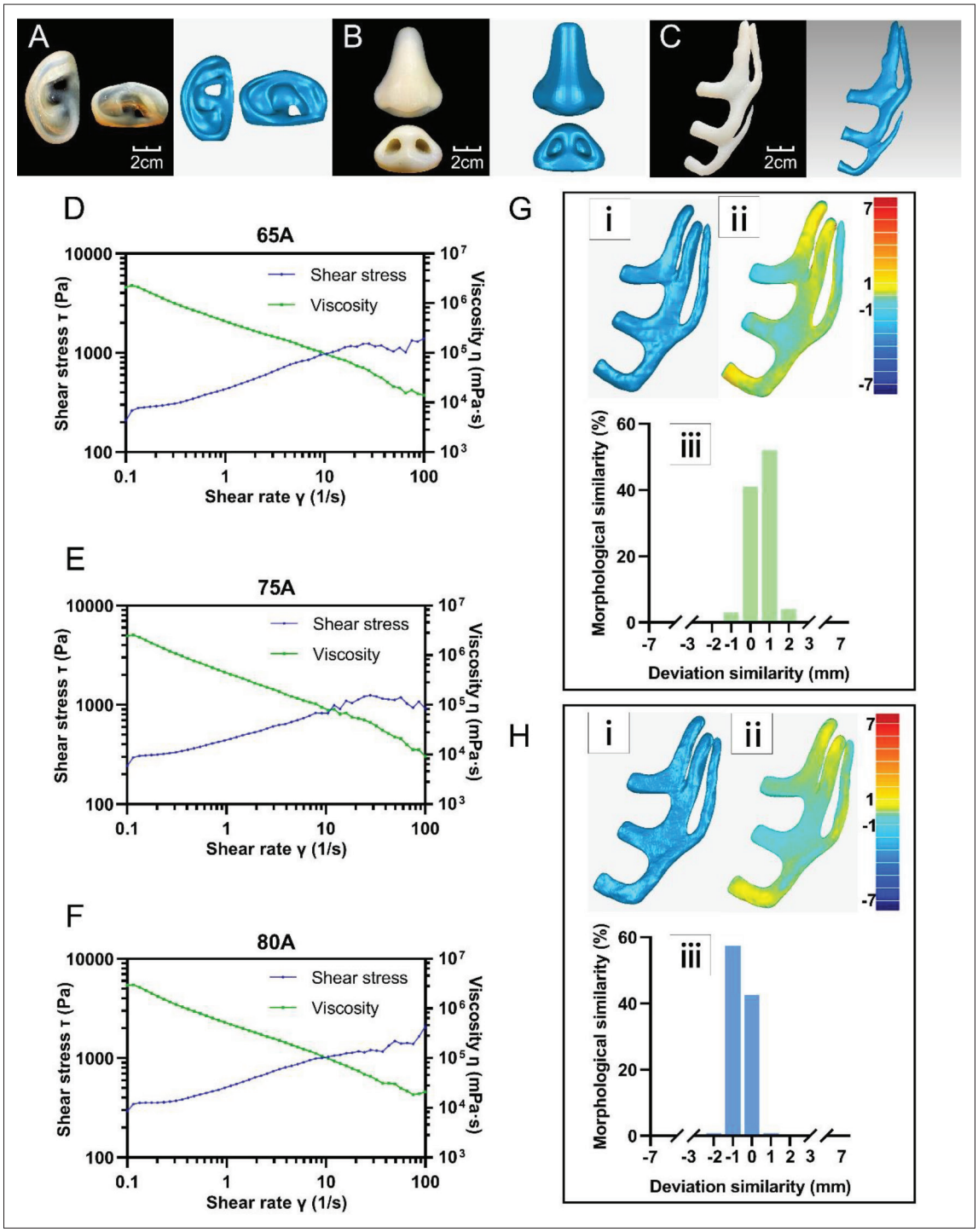

Figure 4. Printability and rheological characterization. (A) 3D digital and 3D-printed silicone auricular model. (B) 3D digital and 3D-printed silicone nasal model. (C) 3D digital and 3D-printed silicone costal cartilage model. Effect of shear rate on viscosity and shear rate versus stress for 65 A (D), 75 A (E), and 80 A (F). (G) Printing trueness of the 3D-printed silicone model. (H) Printing precision of the 3D-printed silicone model.

printing structure, electrostatic attraction between the printed part and extrudate, clogging from in-nozzle curing, and accumulation of nozzle material, which may lead to a decrease in fidelity, making it difficult to perfectly copy the 3D template structure[62,63]. Some studies even suggest that the fidelity of 3D-printed constructs may be even lower than their traditional counterparts[64,65]. Therefore, we performed a 3D scan of the printed constructs to assess

the fidelity of 3D-printed models. Trueness (the deviation from the reference) and precision (the deviation from repeated measurements in the same group) were quantified through 3D deviation comparison of the 3D-printed models reconstructed by CT data. Printing trueness was displayed in the form of a deviation chromatogram, and the deviation within ±1 mm reached 96.40% (Figure 4G), ranging from 87.20% to 96.50%. The deviation of printing precision within ±1 mm reached 99.69% (Figure 4H), ranging from 97.64% to 100%. These results indicated that the printing fidelity was nearly perfect. The addition of a moderator prolongs the time for curing and prevents the emergence of in-nozzle curing. The suitable proportions of thixotropic agents and gas-phase silica in this formula provide good shear-thinning properties for silicone so that printed constructs retain their shape without immediate post-curing[25,66]. In addition, the supporting material prevents collapse and deformation caused by gravity.

3.3. Ear framework handcrafting curricula and individually tailored surgical plans

It is reasonable that patients expect utmost proficiency and mastery from their plastic surgeons. Additionally, the assignment of works to the residents depends on the complexity of the procedure, the patient's condition, and the senior surgeons' disposition toward entrusting the residents with the role of primary surgeon[67]. The high public expectation of perfect patient outcomes and the public awareness of surgeon-specific performance further limit the residents' opportunities to learn by performing procedures in the operating room. Fortunately, 3D-printed models provide a valuable opportunity to learn outside the operating room. As shown in Figure 5A–C, residents who practice on 3D-printed models experienced fast progress. After six training sessions, they spent 55.50 ± 11.42 min on the final attempt compared to 133.30 ± 12.35 min on the first attempt, and the difference was statistically significant ($p < 0.0001$). Overall learner pre-training confidence improved from ratings of 1.60 ± 0.70 to 4.2 ± 0.79 after seven handcrafting attempts (Figure 5D). The average improvement in confidence rating was 2.60 ± 0.97. The printed models improved the learning efficiency of residents through deliberate practice and timely feedback, which is comparable to findings involving our previous indirectly printed models in terms of reduced study time and improved residents' confidence[16]. Table 1 demonstrates the subjective perception of surgeons who attempted 3D-printed costal cartilage models, and the 65 A material received the best feedback. In the subjective evaluation, the three formulations of 3DP silicone all achieved good results, but the 65 A and 75 A materials were the better choice with no significant difference (Figure 5E). According to the surgeons' feedback, the weakness in suture retention ability in the 80 A material resulted in unexpected gaps when assembling the stents with wires, which was related to a decrease in tensile strength for a higher concentration of silica[68]. The application of this kind of costal cartilage model with high satisfaction is expected to greatly shorten the training period of residents.

We performed pre-operative planning using the 3D-printed models on several patients eligible for inclusion in this study, and herein, we showed one of the typical framework carving designs. The 6th, 7th, and 8th costal cartilages were routinely harvested for the majority of ear reconstruction surgeries. However, through the printed models and pre-operative simulations, we found that the patient's 8th costal cartilage was well developed and of sufficient length to replace the 6th (Figure 6A and B), and only the 7th and 8th costal cartilages were harvested during the operation (Figure 6). Good surgical results were still obtained, and the dimensions of cartilage and silicone ear frameworks are shown in **Table S5** (Supplementary File). The differences were not statistically significant ($p = 0.21$). Pertinently, harvesting costal cartilage is one of the essential steps of ear reconstruction surgery, and it inevitably gives rise to multiple complications, including infection, pain, pneumothorax, and chest deformity[69]. The classical scheme needs to collect three or four costal cartilages[70,71], which often leads to wastage of cartilage. During the operation, the remaining cartilage after the fabrication of the cartilage framework can be put back into the donor site[71], but this will still cause unnecessary damage. Thus, pre-operational evaluation of the costal cartilage condition and reducing the amount of harvested cartilage by means of simulated operation is one of the best solutions. 3D-printed models display with fine fidelity the complex anatomical structures of costal cartilage and enable a comprehensive evaluation of the surgical plan that other methods cannot achieve[16]. By applying these models pre-operatively, fabrication simulation allows for a more intuitive evaluation of the cartilage and aids in the determination of the proper amount of cartilage to be harvested for grafting, thereby minimizing the need for excessive logging and identifying potential shortcomings or complications before applying the procedures to patients. Reduced surgical trauma and a potential decrease in the occurrence of chest wall deformity[72,73] are benefits of fewer extracted grafts. This is extremely important for surgeons who lack rich experience in ear reconstruction because they can repeatedly perform ear framework carving exercises for specific patients before surgery, which is of great benefit as it can increase surgical confidence and be used to develop strategies that save time and deliver optimum postoperative results[74]. Based on the same logic, senior surgeons could also benefit from individualized models. Senior surgeons are challenged

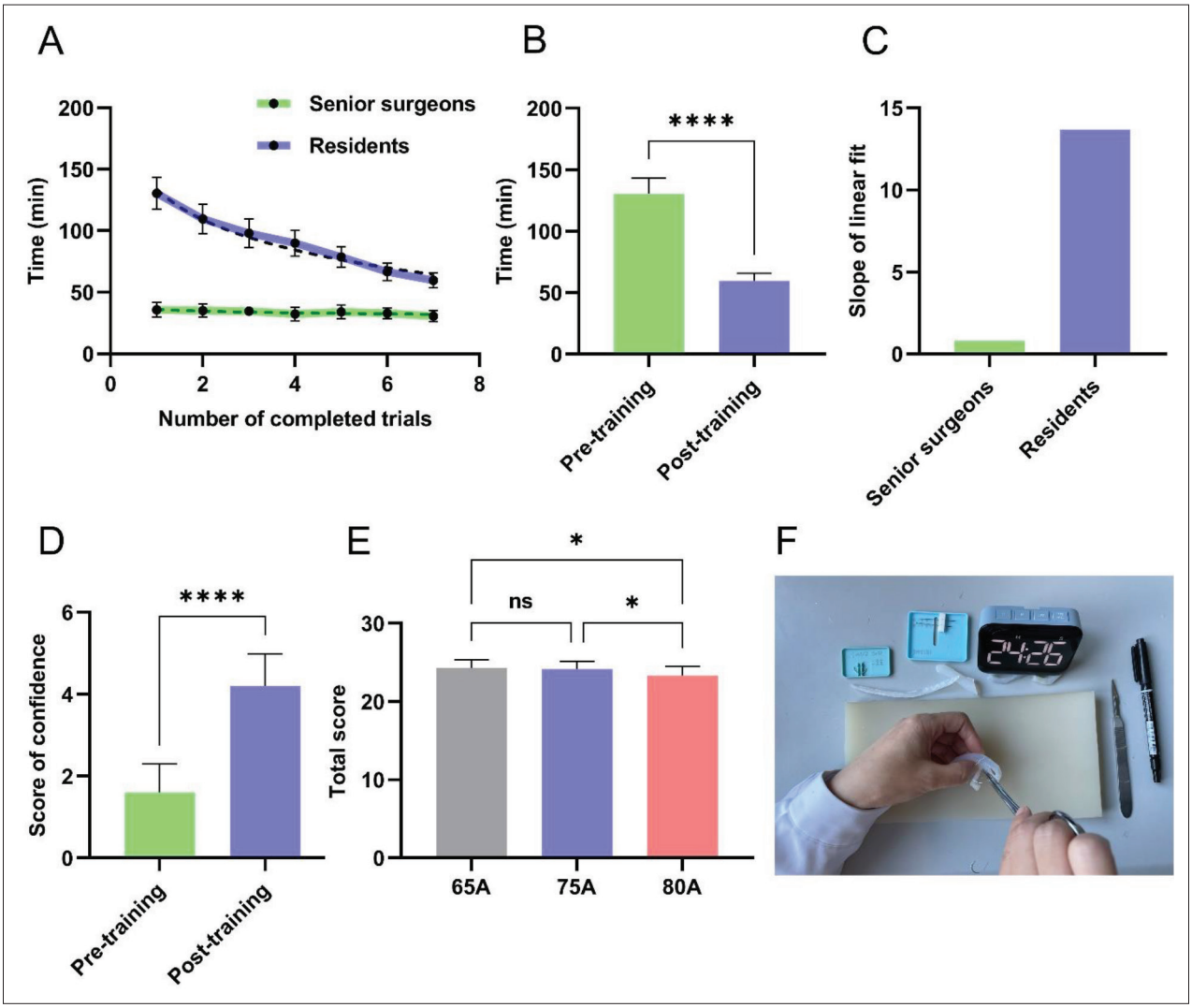

Figure 5. Ear framework handcrafting curricula. (A) Learning curves of senior surgeons and residents applying 3D-printed models. (B) Handcrafting time spent by residents in pre-training and post-training. (C) Quantified slope of the linear fit of learning curves for senior surgeons and residents. (D) Total score of handcrafting confidence among 10 learners in pre-training and post-training. (E) Total score of the subjective perception of surgeons. (F) A senior surgeon was demonstrating how to fabricate an ear framework with a printed model.
Notes: ns, no significant difference; $^{*}p < 0.05$; $^{****}p < 0.0001$

to perform operations for patients with more complex conditions, such as calcification of costal cartilage and failed reconstructed ears[75]. The pre-operative simulation could improve success rates and release physicians' pressure stemming from the complex condition and patients' high expectations. In addition, customized models that have a patient's anatomic structures in the pre-operative setting, as well as in a modified fashion to simulate postoperative conditions, will be valuable for providing pre-operative counseling. Simulation of the operation provides patients with a better understanding of the intended procedures and outcomes[76]. Additionally, the utilization of these models in simulation presents an optimal means for developing and assessing innovative surgical methodologies, thereby facilitating enhanced proliferation of the technology and exchange of ideas among centers and surgeons.

After comprehensively considering the results of both the subjective and objective evaluation, the 75 A material is considered the best option for manufacturing costal cartilage models. Through the model development technology of this study, we can print high-fidelity costal cartilage models for each patient using only a few dollars' worth of material. However, the additional cost (tens of thousands of US dollars) required to purchase devices may limit their widespread use in hospitals, and another

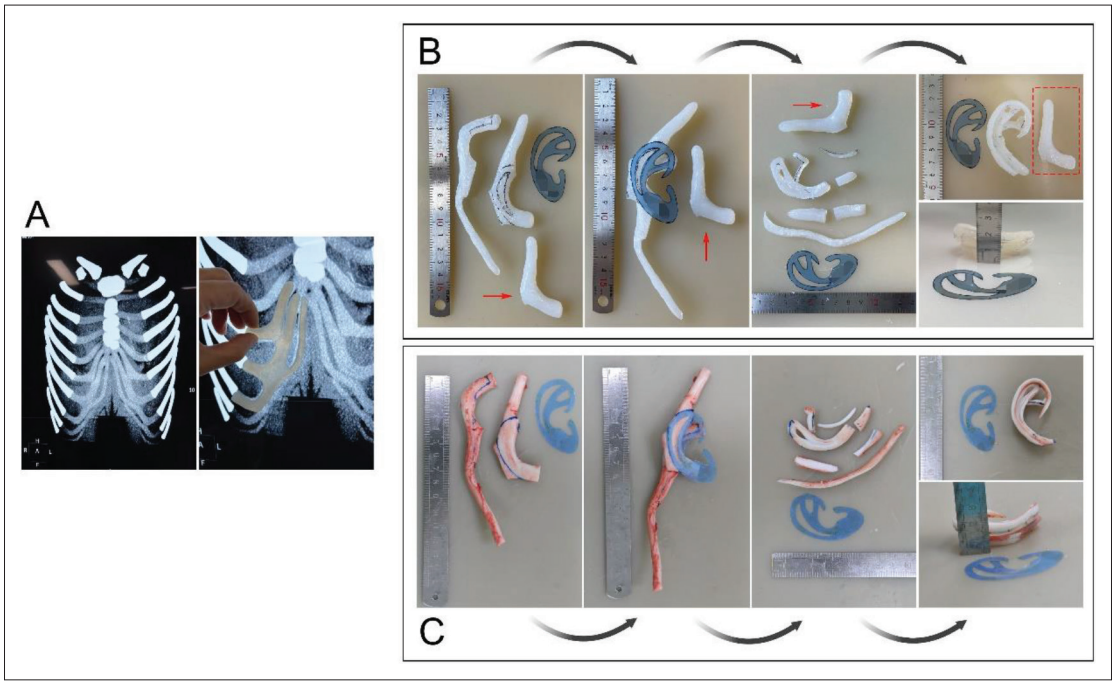

Figure 6. Pre-operative simulation. (A) Individualized 3D-printed silicone model. Pre-operative (B) and intraoperative (C) design of the ear framework. The red arrows and dashed-line box mark the sixth costal cartilage that was spared in the simulation. The patient's name is hidden by a mosaic.

limitation is the manufacturing time, which usually takes several hours after 3D reconstruction to obtain a final model.

3D reconstruction is the most time-consuming process in this technique because the gray level of the costal cartilage is close to that of the surrounding soft tissue, and the image quality is affected by the scanning layer thickness and sharpness. To acquire accurate and objective costal cartilage reconstruction data, operators must change the segmentation's contrast according to their experience after several failures, which require many complicated automatic, semiautomatic, and manual methods. Of course, with the improvement of operating proficiency by gaining experience, the operating time can be reduced from more than 2 hours to approximately 30 min[77], and machine learning is expected to be a useful tool for automatic segmentation and reconstruction of the digital model of costal cartilage.

4. Conclusion

In summary, the current study presents the largest investigation to date of the mechanical properties of costal cartilage in microtia patients and demonstrates that the 75 A material is the best costal cartilage simulation material among three silicone materials. By developing printable silicone formulations that closely match the mechanical properties of costal cartilage and evaluating printing outcomes, the study successfully demonstrated the high fidelity of applying 3D-printing technology to costal cartilage manufacturing. The use of printable silicone and 3D techniques to fabricate costal cartilage models proved highly effective in optimizing the surgical plan through personalized pre-operative simulation. Both mechanical features and subjective evaluations demonstrated that 3D-printed costal cartilage models provided an excellent tool for surgical education, training, and pre-operative simulation of ear frameworks, as well as the potential for nose grafts and other cartilage-related prosthetic fabrication in the plastic surgery field. We considered that the promotion of 3D-printable models in more centers has the potential to improve the learning curves of residents and the overall surgery outcomes.

Acknowledgments

None.

Funding

This work was supported by the National Major Disease Multidisciplinary Diagnosis and Treatment Cooperation Project [21025] and Beijing Municipal Science & Technology Commission [Z221100007422084].

Conflict of interest

The authors declare no conflicts of interests.

Author contributions

Conceptualization: Senmao Wang, Di Wang
Data curation: Senmao Wang, Qian Wang
Formal analysis: Senmao Wang
Funding acquisition: Haiyue Jiang, Lin Lin
Investigation: Senmao Wang, Di Wang, Yuanzhi Yue, Genli Wu, Qian Wang
Methodology: Senmao Wang, Di Wang
Project administration: Lin Lin, Yuyun Chu
Resources: Lin Lin, Haiyue Jiang, Bo Pan, Liya Jia, Yuanzhi Yue, Genli Wu, Yuyun Chu
Supervision: Lin Lin, Haiyue Jiang
Validation: Lin Lin, Liya Jia
Visualization: Senmao Wang
Writing – original draft: Senmao Wang
Writing – review & editing: Di Wang

Ethics approval and consent to participate

Ethical approval of the study was obtained from the institutional review board of the Plastic Surgery Hospital of Chinese Academic of Medical Science and Peking Union Medical College, Beijing, China [Serial number 2023(59)]. Written consent was obtained from each of the subjects to participate in the study.

Consent for publication

Written consent was obtained from each of the subjects to publish their data and images.

Availability of data

Data can be available for readers upon reasonable request.

References

1. Pan B, Jiang H, Guo D, *et al.*, 2008, Microtia: Ear reconstruction using tissue expander and autogenous costal cartilage. *J Plast Reconstr Aesthet Surg,* 61(Suppl 1): S98–S103.

   https://doi.org/10.1016/j.bjps.2007.07.012

2. Zhang Y, Jiang H, Yang Q, *et al.*, 2018, Microtia in a chinese specialty clinic population: clinical heterogeneity and associated congenital anomalies. *Plast Reconstr Surg*, 142(6): 892e–903e.

   https://doi.org/10.1097/prs.0000000000005066

3. Jiang H, Pan B, Lin L, *et al.*, 2008, Fabrication of three-dimensional cartilaginous framework in auricular reconstruction. *J Plast Reconstr Aesthet Surg,* 61(Suppl 1): S77–S85.

   https://doi.org/10.1016/j.bjps.2008.07.007

4. Tanzer RC, 1959, Total reconstruction of the external ear. *Plast Reconstr Surg Transplant Bull,* 23(1): 1–15.

   https://doi.org/10.1097/00006534-195901000-00001

5. Smith RM, Byrne PJ, 2019, Reconstruction of the ear. *Facial Plast Surg Clin North Am,* 27(1): 95–104.

   https://doi.org/10.1016/j.fsc.2018.08.010

6. Kneebone R, 2003, Simulation in surgical training: Educational issues and practical implications. *Med Educ,* 37(3): 267–277.

   https://doi.org/10.1046/j.1365-2923.2003.01440.x

7. Wilkes GH, 2009, Learning to perform ear reconstruction. *Facial Plast Surg,* 25(3): 158–163.

   https://doi.org/10.1055/s-0029-1239452

8. Agrawal K, 2015, Bovine cartilage: A near perfect training tool for carving ear cartilage framework. *Cleft Palate Craniofac J,* 52(6): 758–760.

   https://doi.org/10.1597/14-079r

9. Vadodaria S, Mowatt D, Giblin V, *et al.*, 2005, Mastering ear cartilage sculpture: The vegetarian option. *Plast Reconstr Surg,* 116(7): 2043–2044.

   https://doi.org/10.1097/01.prs.0000192399.15346.23

10. Shin HS, Hong SC, 2013, A porcine rib cartilage model for practicing ear-framework fabrication. *J Craniofac Surg,* 24(5): 1756–1757.

    https://doi.org/10.1097/SCS.0b013e3182902548

11. Erdogan B, Morioka D, Hamada T, *et al.*, 2018, Use of a plastic eraser for ear reconstruction training. *Indian J Plast Surg,* 51(1): 66–69.

    https://doi.org/10.4103/ijps.IJPS_18_18

12. Wu G, Lu L, Ci Z, *et al.*, 2022, Three-dimensional cartilage regeneration using engineered cartilage gel with a 3D-printed polycaprolactone framework. *Front Bioeng Biotechnol*, 10: 871508.

    https://doi.org/10.3389/fbioe.2022.871508

13. Berens AM, Newman S, Bhrany AD, *et al.*, 2016, Computer-aided design and 3D printing to produce a costal cartilage model for simulation of auricular reconstruction. *Otolaryngol Head Neck Surg,* 155(2): 356–359.

    https://doi.org/10.1177/0194599816639586

14. Miyamoto J, Miyamoto S, Nagasao T, *et al.*, 2011, Preoperative modeling of costal cartilage for the auricular reconstruction of microtia. *Plast Reconstr Surg,* 128(1): 23e–24e.

    https://doi.org/10.1097/PRS.0b013e31821744eb

15. Yamada A, Imai K, Fujimoto T, *et al.*, 2009, New training method of creating ear framework by using precise copy of costal cartilage. *J Craniofac Surg,* 20(3): 899–902.

    https://doi.org/10.1097/scs.0b013e3181a2ef97

16. Wang D, Lin L, Yang Q, *et al.*, 2023, Structure and mechanical performance biomimetic costal cartilage models for ear framework handcraft simulation. *Plast Reconstr Surg.*

    https://doi.org/10.1097/prs.0000000000010431

17. Gabrysz-Forget F, Rubin S, Nepomnayshy D, *et al.*, 2020, Development and validation of a novel surgical simulation for parotidectomy and facial nerve dissection. *Otolaryngol Head Neck Surg*, 163(2): 344–347.

https://doi.org/10.1177/0194599820913587

18. Lee M, Ang C, Andreadis K, *et al.*, 2021, An open-source three-dimensionally printed laryngeal model for injection laryngoplasty training. *Laryngoscope,* 131(3): E890–E895.

https://doi.org/10.1002/lary.28952

19. Riedle H, Burkhardt AE, Seitz V, *et al.*, 2019, Design and fabrication of a generic 3D-printed silicone unilateral cleft lip and palate model. *J Plast Reconstr Aesthet Surg,* 72(10): 1669–1674.

https://doi.org/10.1016/j.bjps.2019.06.030

20. Giannopoulos AA, Mitsouras D, Yoo SJ, *et al.*, 2016, Applications of 3D printing in cardiovascular diseases. *Nat Rev Cardiol*, 13(12): 701–718.

https://doi.org/10.1038/nrcardio.2016.170

21. Lim KH, Loo ZY, Goldie SJ, *et al.*, 2016, Use of 3D printed models in medical education: A randomized control trial comparing 3D prints versus cadaveric materials for learning external cardiac anatomy. *Anat Sci Educ*, 9(3): 213–221.

https://doi.org/10.1002/ase.1573

22. Little SH, Vukicevic M, Avenatti E, *et al.*, 2016, 3D printed modeling for patient-specific mitral valve intervention: Repair with a clip and a plug. *JACC Cardiovasc Interv*, 9(9): 973–975.

https://doi.org/10.1016/j.jcin.2016.02.027

23. Liravi F, Toyserkani E, 2018, Additive manufacturing of silicone structures: A review and prospective. *Addit Manuf,* 24: 232–242.

https://doi.org/10.1016/j.addma.2018.10.002

24. Jindal SK, Sherriff M, Waters MG, *et al.*, 2016, Development of a 3D printable maxillofacial silicone: Part I. Optimization of polydimethylsiloxane chains and cross-linker concentration. *J Prosthet Dent*, 116(4): 617–622.

https://doi.org/10.1016/j.prosdent.2016.02.020

25. Jindal SK, Sherriff M, Waters MG, *et al.*, 2018, Development of a 3D printable maxillofacial silicone: Part II. Optimization of moderator and thixotropic agent. *J Prosthet Dent,* 119(2): 299–304.

https://doi.org/10.1016/j.prosdent.2017.04.028

26. Herzberger J, Sirrine JM, Williams CB, *et al.*, 2019, Polymer design for 3D printing elastomers: Recent advances in structure, properties, and printing. *Prog Polym Sci,* 97: 101144.

https://doi.org/10.1016/j.progpolymsci.2019.101144

27. Cevik P, Kocacikli M, 2020, Three-dimensional printing technologies in the fabrication of maxillofacial prosthesis: A case report. *Int J Artif Organs,* 43(5): 343–347.

https://doi.org/10.1177/0391398819887401

28. Cevik P, Akca G, Asar NV, *et al.*, 2023, Antimicrobial effects of nano titanium dioxide and disinfectants on maxillofacial silicones. *J Prosthet Dent,* S0022-3913(23): 00135-X.

https://doi.org/10.1016/j.prosdent.2023.03.001

29. Mannoor MS, Jiang Z, James T, *et al.*, 2013, 3D printed bionic ears. *Nano Lett*, 13(6): 2634–2639.

https://doi.org/10.1021/nl4007744

30. Duoss EB, Weisgraber TH, Hearon K, *et al.*, 2014, Three-dimensional printing of elastomeric, cellular architectures with negative stiffness. *Adv Funct Mater*, 24(31): 4905–4913.

https://doi.org/10.1002/adfm.201400451

31. Mohammed MG, Kramer R, 2017, All-printed flexible and stretchable electronics. *Adv Mater*, 29(19): 1604965.

https://doi.org/10.1002/adma.201604965

32. Sun Y, Wang L, Ni Y, *et al.*, 2023, 3D printing of thermosets with diverse rheological and functional applicabilities. *Nat Commun*, 14(1): 245.

https://doi.org/10.1038/s41467-023-35929-y

33. Femmer T, Kuehne AJ, Wessling M, 2014, Print your own membrane: direct rapid prototyping of polydimethylsiloxane. *Lab Chip,* 14(15): 2610–2613.

https://doi.org/10.1039/c4lc00320a

34. Bhattacharjee N, Parra-Cabrera C, Kim YT, *et al.*, 2018, Desktop-stereolithography 3D-printing of a poly(dimethylsiloxane)-based material with sylgard-184 properties. *Adv Mater,* 30(22): e1800001.

https://doi.org/10.1002/adma.201800001

35. McCoul D, Rosset S, Schlatter S, *et al.*, 2017, Inkjet 3D printing of UV and thermal cure silicone elastomers for dielectric elastomer actuators. *Smart Mater Struct*, 26(12): 125022.

https://doi.org/10.1088/1361-665X/aa9695

36. Liravi F, Vlasea M, 2018, Powder bed binder jetting additive manufacturing of silicone structures. *Addit Manuf,* 21: 112–124.

https://doi.org/10.1016/j.addma.2018.02.017

37. Liravi F, Toyserkani E, 2018, Additive manufacturing of silicone structures: A review and prospective. *Addit Manuf,* 24: 232–242.

https://doi.org/10.1016/j.addma.2018.10.002

38. Zhang Y, Huang F, Zhang E, *et al.*, 2023, Effect of the support bath on embedded 3D printing of soft elastomeric composites. *Mater Lett,* 331: 133475.

https://doi.org/10.1016/j.matlet.2022.133475

39. Chen S, Tan WS, Bin Juhari MA, *et al.*, 2020, Freeform 3D printing of soft matters: Recent advances in technology for biomedical engineering. *Biomed Eng Lett,* 10(4): 453–479.

    https://doi.org/10.1007/s13534-020-00171-8

40. Wu W, DeConinck A, Lewis JA, 2011, Omnidirectional printing of 3D microvascular networks. *Adv Mater,* 23(24): H178–H183.

    https://doi.org/10.1002/adma.201004625

41. O'Bryan CS, Bhattacharjee T, Hart S, *et al.*, 2017, Self-assembled micro-organogels for 3D printing silicone structures. *Sci Adv,* 3(5): e1602800.

    https://doi.org/10.1126/sciadv.1602800

42. Landers R, Mülhaupt R, 2000, Desktop manufacturing of complex objects, prototypes and biomedical scaffolds by means of computer-assisted design combined with computer-guided 3D plotting of polymers and reactive oligomers. *Macromol Mater Eng,* 282(1): 17–21.

    https://doi.org/10.1002/1439-2054(20001001)282:1<17::AID-MAME17>3.0.CO;2-8

43. Zhao J, Hussain M, Wang M, *et al.*, 2020, Embedded 3D printing of multi-internal surfaces of hydrogels. *Addit Manuf,* 32: 101097.

    https://doi.org/10.1016/j.addma.2020.101097

44. Truby RL, Wehner M, Grosskopf AK, *et al.*, 2018, Soft somatosensitive actuators via embedded 3D printing. *Adv Mater,* 30(15): e1706383.

    https://doi.org/10.1002/adma.201706383

45. Calais T, Sanandiya ND, Jain S, *et al.*, 2022, Freeform liquid 3D printing of soft functional components for soft robotics, *ACS Appl Mater Interfaces,* 14(1): 2301–2315.

    https://doi.org/10.1021/acsami.1c20209

46. Karyappa R, Ching T, Hashimoto M, 2020, Embedded ink writing (EIW) of polysiloxane inks. *ACS Appl Mater Interfaces,* 12(20): 23565–23575.

    https://doi.org/10.1021/acsami.0c03011

47. Muth JT, Vogt DM, Truby RL, *et al.*, 2014, Embedded 3D printing of strain sensors within highly stretchable elastomers. *Adv Mater,* 26(36): 6307–6312.

    https://doi.org/10.1002/adma.201400334

48. Szarko M, Muldrew K, Bertram JE, 2010, Freeze-thaw treatment effects on the dynamic mechanical properties of articular cartilage. *BMC Musculoskelet Disord*, 11: 231.

    https://doi.org/10.1186/1471-2474-11-231

49. Griffin MF, O'Toole G, Sabbagh W, *et al.*, 2020, Comparison of the compressive mechanical properties of auricular and costal cartilage from patients with microtia. *J Biomech,* 103: 109688.

    https://doi.org/10.1016/j.jbiomech.2020.109688

50. Pensalfini M, Meneghello S, Lintas V, *et al.*, 2018, The suture retention test, revisited and revised. *J Mech Behav Biomed Mater,* 77: 711–717.

    https://doi.org/10.1016/j.jmbbm.2017.08.021

51. Sheckter CC, Kane JT, Minneti M, *et al.*, 2013, Incorporation of fresh tissue surgical simulation into plastic surgery education: maximizing extraclinical surgical experience. *J Surg Educ,* 70(4): 466–474.

    https://doi.org/10.1016/j.jsurg.2013.02.008

52. Howard GS, 1980, Response-shift bias: A problem in evaluating interventions with pre/post self-reports. *Eval Rev,* 4(1): 93–106.

    https://doi.org/10.1177/0193841X8000400105

53. Jiang H, Pan B, Zhao Y, *et al.*, 2011, A 2-stage ear reconstruction for microtia. *Arch Facial Plast Surg,* 13(3): 162–166.

    https://doi.org/10.1001/archfacial.2011.30

54. Grellmann W, Berghaus A, Haberland EJ, *et al.*, 2006, Determination of strength and deformation behavior of human cartilage for the definition of significant parameters. *J Biomed Mater Res A,* 78(1): 168–174.

    https://doi.org/10.1002/jbm.a.30625

55. Wang X, Dong W, Wang H, *et al.*, 2023, Mechanical properties of extensive calcified costal cartilage: An experimental study. *Heliyon*, 9(2): e13656.

    https://doi.org/10.1016/j.heliyon.2023.e13656

56. Weber M, Rothschild MA, Niehoff A, 2021, Anisotropic and age-dependent elastic material behavior of the human costal cartilage. *Sci Rep,* 11(1): 13618.

    https://doi.org/10.1038/s41598-021-93176-x

57. Levental I, Georges PC, Janmey PA, 2007, Soft biological materials and their impact on cell function. *Soft Matter,* 3(3): 299–306.

    https://doi.org/10.1039/b610522j

58. Lau AG, Kindig MW, Salzar RS, *et al.*, 2015, Micromechanical modeling of calcifying human costal cartilage using the generalized method of cells. *Acta Biomater,* 18: 226–235.

    https://doi.org/10.1016/j.actbio.2015.02.012

59. Sunwoo WS, Choi HG, Kim DW, *et al.*, 2014, Characteristics of rib cartilage calcification in Asian patients. *JAMA Facial Plast Surg,* 16(2): 102–106.

    https://doi.org/10.1001/jamafacial.2013.2031

60. Baumgart E, 2000, Stiffness--an unknown world of mechanical science?, *Injury,* 31(Suppl 2): S–B14–23.

    https://doi.org/10.1016/S0020-1383(00)80040-6

61. Zhang Y, Liu W, Zhou Q, *et al.*, 2023, Effects of vinyl functionalized silica particles on thermal and mechanical

properties of liquid silicone rubber nanocomposites. *Polymers,* 15(5): 1224.

https://doi.org/10.3390/polym15051224

62. In E, Walker E, Naguib HE, 2017, Novel development of 3D printable UV-curable silicone for multimodal imaging phantom. *Bioprinting*, 7: 19–26.

https://doi.org/10.1016/j.bprint.2017.05.003

63. Porter D, Cohen A, Krueger P, *et al.*, 2018, Additive manufacturing with ultraviolet curable silicones containing carbon black. *3D Print Addit Manuf,* 5: 73–86.

https://doi.org/10.1089/3dp.2017.0019

64. Sim JY, Jang Y, Kim WC, *et al.*, 2019, Comparing the accuracy (trueness and precision) of models of fixed dental prostheses fabricated by digital and conventional workflows. *J Prosthodont Res,* 63(1): 25–30.

https://doi.org/10.1016/j.jpor.2018.02.002

65. Jin SJ, Kim DY, Kim JH, *et al.*, 2019, Accuracy of dental replica models using photopolymer materials in additive manufacturing: in vitro three-dimensional evaluation. *J Prosthodont,* 28(2): e557–e562.

https://doi.org/10.1111/jopr.12928

66. Durban MM, Lenhardt JM, Wu AS, *et al.*, 2018, Custom 3D printable silicones with tunable stiffness. *Macromol Rapid Commun,* 39(4): 1700563.

https://doi.org/10.1002/marc.201700563

67. Yoo SJ, Hussein N, Barron DJ, 2022, Congenital heart surgery skill training using simulation models: Not an option but a necessity. *J Korean Med Sci,* 37(38): e293.

https://doi.org/10.3346/jkms.2022.37.e293

68. Chiulan I, Panaitescu DM, Radu ER, *et al.*, 2020, Comprehensive characterization of silica-modified silicon rubbers. *J Mech Behav Biomed Mater,* 101: 103427.

https://doi.org/10.1016/j.jmbbm.2019.103427

69. Lonergan AR, Scott AR, 2020, Autologous costochondral graft harvest in children. *Int J Pediatr Otorhinolaryngol,* 135: 110111.

https://doi.org/10.1016/j.ijporl.2020.110111

70. Tanzer RC, 1978, Microtia--a long-term follow-up of 44 reconstructed auricles. *Plast Reconstr Surg,* 61(2): 161–166.

https://doi.org/10.1097/00006534-197802000-00001

71. Kawanabe Y, Nagata S, 2006, A new method of costal cartilage harvest for total auricular reconstruction: Part I. Avoidance and prevention of intraoperative and postoperative complications and problems. *Plast Reconstr Surg,* 117(6): 2011–2018.

https://doi.org/10.1097/01.prs.0000210015.28620.1c

72. Dong W, Song Y, Jiang H, *et al.*, 2020, Method of reducing thoracic deformity in auricular reconstruction. *J Craniofac Surg,* 31(2): 520–521.

https://doi.org/10.1097/scs.0000000000006172

73. Thomson HG, Kim TY, Ein SH, 1995, Residual problems in chest donor sites after microtia reconstruction: A long-term study. *Plast Reconstr Surg,* 95(6): 961–968.

https://doi.org/10.1097/00006534-199505000-00002

74. Cornejo J, Cornejo-Aguilar JA, Vargas M, *et al.*, 2022, Anatomical engineering and 3D printing for surgery and medical devices: International review and future exponential innovations. *Biomed Res Int,* 2022: 6797745.

https://doi.org/10.1155/2022/6797745

75. Yue X, Jiang H, Pan B, *et al.*, 2022, Secondary surgery for the unsatisfactory auricle after auricular reconstruction. *Int J Pediatr Otorhinolaryngol*, 154: 111043.

https://doi.org/10.1016/j.ijporl.2022.111043

76. Wang Q, Wang Y, Zhou X, *et al.*, 2022, Three-dimensional auricular subunit models for cartilage framework fabrication: Our preliminary experience. *J Craniofac Surg,* 33(4): 1111–1115.

https://doi.org/10.1097/scs.0000000000008163

77. Cai T, Rybicki FJ, Giannopoulos AA, *et al.*, 2015, The residual STL volume as a metric to evaluate accuracy and reproducibility of anatomic models for 3D printing: application in the validation of 3D-printable models of maxillofacial bone from reduced radiation dose CT images. *3D Print Med,* 1(1): 2.

https://doi.org/10.1186/s41205-015-0003-3